Simultaneous model predictive control and moving horizon estimation for blood glucose regulation in Type 1 diabetes

Article *in* Optimal Control Applications and Methods · November 2017

DOI: 10.1002/oca.2388

CITATIONS
25

READS
295

3 authors, including:

David A. Copp
University of California, Irvine
49 PUBLICATIONS **0** CITATIONS
SEE PROFILE

Joao P. Hespanha
University of California, Santa Barbara
581 PUBLICATIONS **0** CITATIONS
SEE PROFILE

OPTIMAL CONTROL APPLICATIONS AND METHODS
Optim. Control Appl. Meth. 2016; **00**:1–15
Published online in Wiley InterScience (www.interscience.wiley.com). DOI: 10.1002/oca

Simultaneous Model Predictive Control and Moving Horizon Estimation for Blood Glucose Regulation in Type 1 Diabetes

David A. Copp[1]*, Ravi Gondhalekar[1], and João P. Hespanha[1]

[1] *University of California, Santa Barbara, CA 93106, U.S.A.*

SUMMARY

A new estimation and control approach for the feedback control of an artificial pancreas to treat type 1 diabetes mellitus is proposed. In particular, we present a new output feedback predictive control approach that simultaneously solves the state estimation and control objectives by means of a single min-max optimization problem. This involves optimizing a cost function with both finite forward and backward horizons with respect to the unknown initial state, unmeasured disturbances and noise, and future control inputs, and is similar to simultaneously solving a Model Predictive Control (MPC) problem and a Moving Horizon Estimation (MHE) problem. We incorporate a novel asymmetric output cost in order to penalize dangerous low blood-glucose values more severely than less harmful high blood-glucose values. We compare this combined MPC/MHE approach to a control strategy that uses state-feedback MPC preceded by a Luenberger observer for state estimation. *In-silico* results showcase several advantages of this new simultaneous MPC/MHE approach, including fewer hypoglycemic events without increasing the number of hyperglycemic events, faster insulin delivery in response to meal consumption, and shorter insulin pump suspensions, resulting in smoother blood-glucose trajectories.

Received . . .

KEY WORDS: model predictive control; moving horizon estimation; output feedback control; control of constrained systems; optimal control; optimal estimation; artificial pancreas.

1. INTRODUCTION

Type 1 Diabetes Mellitus (T1DM) is a metabolic auto-immune disease that destroys pancreatic β-cells, making it impossible for the pancreas to produce insulin, a hormone the body uses to regulate glucose levels in the blood stream and to facilitate the absorption of glucose into many types of cells. Because of this, people with T1DM require monitoring of Blood-Glucose (BG) levels and delivery of insulin from an external source. If BG levels are not regulated well, people with T1DM suffer from hyperglycemia and hypoglycemia (high and low BG levels, respectively), which can cause severe health problems. An individual who experiences hyperglycemia over long periods of time may, for example, eventually experience cardiovascular disease, kidney failure, and retinal damage, possibly after many years. Hypoglycemia, on the other hand, may have immediate consequences ranging from dizziness and unconsciousness to possibly even coma or death.

Much recent research has been devoted to the feedback control of an Artificial Pancreas (AP) in order to reduce the burden and improve the effectiveness of T1DM treatment by automating the dosing and delivery of insulin [1, 2, 3]. In the AP, it is the job of a feedback controller to determine appropriate amounts of insulin to be delivered given measurements of BG levels, and

*Correspondence to: E-mail: dacopp@ucsb.edu

these closed-loop algorithms have been shown to be much more effective than open-loop insulin administration in both simulation and clinical trials [4, 5, 6, 7]. This work focuses on control of an AP that delivers insulin using a Continuous Subcutaneous Insulin Infusion (CSII) pump and receives BG measurements based on a Continuous Glucose Monitor (CGM) [8], as is the case with AP units destined for outpatient use. Given the potentially severe consequences of excessive or insufficient insulin delivery, the algorithms for feedback control of an AP are crucial for the successful treatment of T1DM [3, 9].

One of the most popular control approaches for the delivery of insulin using an AP is Model Predictive Control (MPC) [10, 11, 12]. Given a model of the plant to be controlled and the current state of the plant, MPC involves solving an online optimization problem over a future time horizon. This yields a sequence of optimal control inputs to be applied to the plant in the future as well as predicted states of the plant based on these inputs [13, 14]. Only the first element of the computed input sequence is applied as an input to the plant, and at each sampling time, this technique is repeated. MPC has been one of the most successful advanced control methods in many industries, including the feedback control of an AP, because of its ability to explicitly handle hard state and input constraints. For a survey of MPC applications in industry, see [15].

Classic MPC is formulated assuming full-state feedback. However, this is not practical in most control problems where only noisy measurements of the state are available. Therefore, a state estimation scheme is needed to accompany the state feedback controller. Indeed, when designing a feedback controller for an AP, only measurements of a person's BG from a CGM, which contain noise and delays, are available, so a state estimation strategy is required. Examples of algorithms for state estimation include observers, filters, and moving horizon estimation, some of which are discussed in [16]. Some of the authors' past work has involved the use of a Luenberger observer for state estimation with an AP [17, 18, 19, 20]. The performance of this Luenberger observer was compared to that of Moving Horizon Estimation (MHE) in [21], and it was found that MHE provided better state estimates and allowed faster insulin delivery in response to meal consumption. MHE is, in some sense, the dual of MPC and characterizes an estimate of the state by solving an optimization problem in real time. The optimization problem is formulated over past measurements and inputs. The use of online optimization in MHE is attractive because constraints can be accommodated explicitly.

In this work, we utilize a novel combination of MPC with MHE recently proposed in [22, 23]. Specifically, we consider output feedback using a model that explicitly includes additive measurement noise and input disturbances, and formulate the combined MPC and MHE problem as a single min-max optimization over both control inputs (min) and the unknown initial state and input disturbances (max). In this way, we solve both the MPC and MHE objectives simultaneously, which gives us an optimal (in a certain sense) control input sequence at each sampling time for worst-case (in a certain sense) estimates of the current state, disturbances, and noise.

The BG regulation problem exhibits inherent asymmetry, which poses a challenge when designing a controller. The asymmetry stems from the fact that hypoglycemia has more immediate and dire consequences than hyperglycemia, insulin can only be delivered, not removed, and, in the single-hormone AP considered here, there is no control action available for increasing BG. Therefore, responding assertively to hyperglycemia and commanding corrective insulin, but not over-correcting and thereby inducing subsequent hypoglycemia, is a paramount and difficult challenge. Many AP controllers utilize supervisory control or additional safety logic to address this challenge. In this work, we propose an appropriate choice of the MPC cost function to address this challenge with the goal of removing, or at least reducing, the need for additional ad hoc safeguards. Specifically, we consider an asymmetric output cost that penalizes "riskier" low BG values more severely than high BG values. Asymmetric output costs have been considered by others in works such as [12, 24] but with different implementations.

Our proposed output cost function is not only asymmetric but also assigns very low cost to BG values within a safe range in order to regulate BG values to be within that range, rather than tracking a particular set-point, similar to the AP controllers deployed in clinical trials [17, 20, 25]. In this way, our output cost function enforces a small penalty for BG values within a desired range and

DOI: 10.1002/oca

sharply (asymmetrically) penalizes excursions outside of that range. This approach has proven useful in AP applications as there exists a set of BG values generally considered to be safe, and it is extremely difficult to obtain accurate physiological models [26, 27, 28]. There is often large plant-model mismatch due to the significant variability in the physiology of a single individual over time as well as due to differences between individuals. It is also difficult to accurately model the noise and delays that are present in the BG measurements provided by a CGM. Therefore, regulating to a range of BG values is one method to prevent excessive response to changes in the measurements when the measured BG level is safely within the desired range.

To demonstrate the differences and benefits of the combined MPC/MHE strategy, in this paper the results are compared to results from a method that has performed successfully in outpatient clinical trials. The method is a state-feedback MPC strategy that utilizes asymmetric input costs and a Luenberger observer for state estimation and is described in [17]. Throughout the paper, we refer to this approach as the MPC/LO method. In [17], the MPC/LO method is augmented with feed-forward control action following user-initiated meal announcement, insulin-on-board constraints [29], diurnal zones and constraints, and other safety features required for clinical trials. One of the goals of this paper is to show that the novel MPC/MHE method has benefits over the MPC/LO method. Towards this goal, we compare the performance of MPC/MHE with that of the basic MPC/LO, and for neither algorithm do we include the safety augmentations mentioned above. While these safety features are currently required for safe execution of an automated system in human clinical trials, we omit them here, first, to enable a more direct comparison between the MPC laws without obscuring those differences with the effects of auxiliary safety mechanisms and, second, in order to not obfuscate the exposition of the paper. For example, it would be useful or even necessary to consider meal announcement or detection for clinical trials; however, even when meal announcement or detection is available a controller must be able to handle the more difficult case of unannounced meals, and meal-boluses and other feed-forward boluses hide or prevent the action of the control law, making it difficult (or irrelevant) to contrast different control laws. We leave preparation of this new control and estimation method for clinical deployment (including the incorporation of such techniques as meal detection [30]) as future work. It is thus important to clarify that the simulation results presented here (for MPC/LO and for MPC/MHE) are not representative of expected results in trials, since these would require additional, above-mentioned safety features.

We demonstrate the benefits of the proposed MPC/MHE approach by presenting *in-silico* studies based on the commercially available 10-subject Universities of Virginia/Padova (UVA/Padova) metabolic simulator accepted by the United States Food and Drug Administration (USFDA) [31]. The *in-silico* results showcase several advantages of the MPC/MHE approach, including fewer hypoglycemic events without increasing the number of hyperglycemic events, faster insulin delivery in response to meal consumption, and shorter insulin pump suspensions, resulting in smoother BG trajectories.

The paper is organized as follows: We present the control-relevant model, desired BG range, and input constraints in Section 2. In Section 3 we describe our combined MPC/MHE estimation and control approach and compare it to a simplified version of the approach from [17] utilizing state-feedback MPC with a Luenberger observer as state estimator. In Section 4 we compare the results of the two estimation and control approaches and discuss the advantages of the MPC/MHE approach. Finally, we conclude with closing remarks in Section 5.

2. PROBLEM FORMULATION

2.1. *Insulin-glucose transfer function*

Because it is difficult to derive accurate models, and because there are long delays and significant noise in the CGM measurements, accurate estimation and effective control for an AP is exceptionally challenging. We use the control-relevant model proposed in [27], which has successfully been employed in AP controller design in [17, 20]. The model is a discrete-time linear time-invariant (LTI) system with sample period $T_s = 5$ minutes. Denoting the current time by t, the

DOI: 10.1002/oca

scalar plant input is the administered insulin bolus $u_{\mathrm{IN},t}$ [U] delivered per sample period, and the scalar plant output is the subject's BG value $y_{\mathrm{BG},t}$ [mg/dL]. The plant is linearized around a steady-state that is assumed to result in a BG output $y_s = 110$ [mg/dL] when applying the subject-specific, basal input rate u_{BASAL} [U/hour].

The input u_t and output y_t of the LTI model are defined as

$$u_t \coloneqq u_{\mathrm{IN},t} - u_{\mathrm{BASAL}} \times \tfrac{T_s}{60\mathrm{min/hour}}, \qquad y_t \coloneqq y_{\mathrm{BG},t} - y_s.$$

Denoting z^{-1} as the backwards shift operator, we write $\mathcal{U}(z^{-1})$ and $\mathcal{Y}(z^{-1})$ for the z-transforms of the time-domain signals of input u_t and output y_t, respectively. The transfer function from u to y is given by

$$\frac{\mathcal{Y}(z^{-1})}{\mathcal{U}(z^{-1})} = \frac{1800g}{u_{\mathrm{TDI}}} \times \frac{z^{-3}}{(1-p_1 z^{-1})(1-p_2 z^{-1})^2} \tag{1}$$

with poles $p_1 = 0.98$, $p_2 = 0.965$, the subject-specific *total daily insulin* amount u_{TDI} [U], and with the constant

$$g \coloneqq -90(1-p_1)(1-p_2)^2$$

employed to set the correct gain and for unit conversion. The number 1800 comes from the "1800 rule" to estimate BG decrease with respect to delivering rapid-acting insulin [32].

2.2. State-space model

For control, we utilize a state-space model of the form

$$x_{t+1} = Ax_t + Bu_t + Dd_t \qquad y_t = Cx_t + n_t, \tag{2}$$

with

$$\begin{aligned} A &\coloneqq \begin{bmatrix} p_1+2p_2 & -2p_1p_2-p_2^2 & p_1p_2^2 \\ 1 & 0 & 0 \\ 0 & 1 & 0 \end{bmatrix} \in \mathbb{R}^{3\times 3} \\ B &\coloneqq \tfrac{1800g}{u_{\mathrm{TDI}}} \begin{bmatrix} 1 & 0 & 0 \end{bmatrix}^\top \in \mathbb{R}^3 \\ D &\coloneqq -B/10 \in \mathbb{R}^3 \\ C &\coloneqq \begin{bmatrix} 0 & 0 & 1 \end{bmatrix} \in \mathbb{R}^{1\times 3}. \end{aligned}$$

The *state* is $x_t \in \mathbb{R}^3$. The inputs are the *control input* u_t that belongs to the set $\mathcal{U} \subset \mathbb{R}$, and the *unmeasured disturbance* d_t that is assumed to belong to a set $\mathcal{D} \subset \mathbb{R}$. The *measurement noise* n_t belongs to the set $\mathcal{N} \subset \mathbb{R}$. The nominal system ((2) without d_t and n_t) is an equivalent realization of (1). We have included noise and disturbance terms n_t and d_t, respectively, in order to explicitly account for model uncertainty, additive disturbances, and sensor noise. The matrix D is chosen to allow the disturbance to affect the state an order of magnitude smaller, and in the opposite way, than the insulin delivered as the control input does. Therefore, a positive disturbance d induces a rise in modeled BG output, akin to the consumption of carbohydrates.

2.3. Desired blood-glucose range

In the MPC/LO approach that we compare with, a range of desired BG values, i.e., the BG values generally considered safe and for which delivering the insulin basal rate is appropriate, is considered. This range is $[\underline{r}, \overline{r}]$ mg/dL, where $\underline{r} = 80$ and $\overline{r} = 140$, the same as in [4, 27]. For simplicity, the range is time-invariant, in contrast to [17, 20]. In order to implement this range in the controller, BG values are penalized according to the range excursion $Z : \mathbb{R} \to \mathbb{R}$ defined as

$$Z(y) \coloneqq \arg\min_{\alpha\in\mathbb{R}} \{\alpha^2 | y + y_s - \alpha \in [\underline{r}, \overline{r}]\}. \tag{3}$$

DOI: 10.1002/oca

For the MPC/MHE approach, we do not penalize BG values based on their excursion from a strictly defined range, but rather approximate the desired range by penalizing BG values according to the following functions $h : \mathbb{R} \to \mathbb{R}$ and $c : \mathbb{R} \to \mathbb{R}$:

$$h(y) \coloneqq (\arctan(0.1y) + \pi/2)y + 10, \qquad c(y) \coloneqq \check{\lambda}h(-y + \underline{r}) + \hat{\lambda}h(y - \overline{r} + 20), \tag{4}$$

where $c(y)$ is parameterized by $\check{\lambda}$, the weight on low BG, and $\hat{\lambda}$, the weight on high BG. These weights can be chosen to separately tune the control response to hypoglycemia and hyperglycemia. In this work, we choose $\check{\lambda} = 0.02$ and $\hat{\lambda} = 0.005$ based on experimentation. The remaining numbers in (4), such as 0.1, $\pi/2$, 10, and 20, are chosen to shift the nominal cost as desired. Plots of these functions h and c are shown in Figure 1. The output cost used in the MPC/MHE cost function (6) below is $c(y)^2$. Therefore, the output cost is asymmetric with respect to the desired BG range, roughly penalizing lower BG values 4^2 times more heavily than higher BG values.

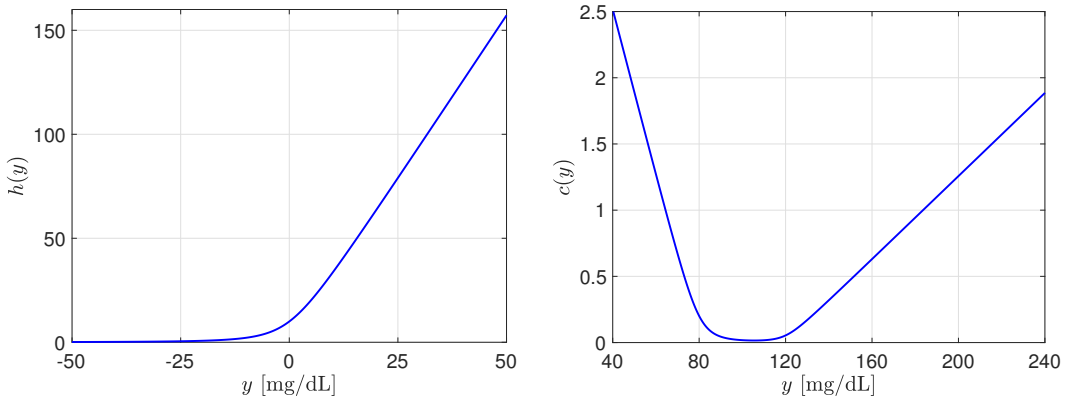

(a) arctan function $h(y)$. (b) Asymmetric function $c(y)$.

Figure 1. Functions defining asymmetric output penalty as defined in (4).

2.4. *Insulin delivery constraints*

At each time t the control input is restricted to the set $\mathcal{U}$ defined as

$$\mathcal{U} \coloneqq \{u_t \in \mathbb{R} | 0 \leqslant u_t + u_{\text{BASAL}} \times \tfrac{T_s}{60\text{min/hour}} \leqslant u_{\text{MAX}}\}, \tag{5}$$

where $u_{\text{MAX}} = 25$ [U] is the maximum bolus size the CSII pump is allowed to command. This upper bound is so large it will not be met during normal operation of an AP, but it is included to safeguard against data problems that may result in anomalously large insulin spikes.

3. ESTIMATION AND CONTROL APPROACH

In this section, we discuss our novel MPC/MHE estimation and control approach and compare it to a control strategy that is based on state-feedback MPC with a Luenberger Observer (MPC/LO). As discussed in the introduction, a more complicated version of this MPC/LO approach augmented with additional safety features has been used in clinical trials, but we use a simplified version as a benchmark-controller in this study. First we define some notation: We denote by $\mathbb{Z}_{\geqslant 0}$ the set of non-negative integers, by $\mathbb{Z}_+$ the set of positive integers, and by $\mathbb{Z}_a^b$ the set of consecutive integers $\{a, ..., b\}$. Given a discrete-time signal $w : \mathbb{Z}_{\geqslant 0} \to \mathbb{R}^n$ and two times t_0, $t \in \mathbb{Z}_{\geqslant 0}$ with $t_0 < t$, we denote by $w_{t_0:t}$ the sequence $\{w_{t_0}, w_{t_0+1}, ..., w_t\}$. The prediction horizon is denoted by $T \in \mathbb{Z}_+$, the control horizon is denoted by $M \in \mathbb{Z}_1^T$, and the estimation horizon is denoted by $L \in \mathbb{Z}_+$. In this work, we choose $T = 9$, $M = 5$, and $L = 3$ (where T and M are chosen the same as in [17], and L was chosen based on experimentation).

DOI: 10.1002/oca

3.1. Combined MPC and MHE

Our estimation and control approach combines MPC and MHE as discussed in [22, 23], where the MPC and MHE optimization objectives are incorporated within a single min-max optimization problem, the solution of which simultaneously characterizes solutions to the MHE and MPC sub-problems. We formulate the MPC/MHE problem as a finite-horizon min-max optimization problem, to be solved at each time t, of the form

$$\min_{u_{t:t+M-1}} \quad \max_{\substack{x_{t-L},\\ d_{t-L:t+T-1}}} \quad J_t(x_{t-L}, u_{t-L:t-1}, u_{t:t+M-1}, d_{t-L:t+T-1}, n_{t-L:t}) \tag{6}$$

with cost function

$$J_t(\cdot) \coloneqq \sum_{k=t+1}^{t+T} c(Cx_k)^2 + \sum_{k=t}^{t+M-1} \lambda_u u_k^2 - \sum_{k=t-L}^{t+T-1} \lambda_d d_k^2 - \sum_{k=t-L}^{t} \lambda_n n_k^2, \tag{7}$$

and subject to

$$x_{k+1} = Ax_k + Bu_k + Dd_k \qquad \forall k \in \mathbb{Z}_{t-L}^{t+T-1} \tag{8a}$$

$$y_k = Cx_k + n_k \qquad \forall k \in \mathbb{Z}_{t-L}^{t} \tag{8b}$$

$$d_k \in \mathcal{D} \qquad \forall k \in \mathbb{Z}_{t-L}^{t+T-1} \tag{8c}$$

$$u_k \in \mathcal{U} \qquad \forall k \in \mathbb{Z}_{t}^{t+M-1} \tag{8d}$$

$$u_k = 0 \qquad \forall k \in \mathbb{Z}_{t+M}^{t+T-1} \tag{8e}$$

where λ_u, λ_d, and λ_n are positive scalar weights on the control input u, disturbance d, and measurement noise n, respectively. In this work, we choose these weights to be $\lambda_u = 2$, $\lambda_d = 2$, and $\lambda_n = 300$. The running cost $c(\cdot)$ is given in (4) and shown in Figure 1(b).

Equations (8a)-(8b) enforce the dynamics of the model (2). Equations (8c) and (8d) enforce that the input disturbance and control input belong to the constraint sets $\mathcal{D}$ and $\mathcal{U}$ (as defined in (5)), respectively. In this work, we define the constraint set $\mathcal{D} \coloneqq \{d \in \mathbb{R} | 0 \leqslant d \leqslant 0.5\}$. A disturbance of $d = 0.5$ would counteract the effects of delivering 0.05 [U] insulin (which turns out to be slightly more than the standard deviation from the mean insulin delivered using the MPC/MHE approach shown later in Figure 3). Lastly, equation (8e) ensures that, beyond the control horizon M, the basal rate u_{BASAL} is delivered.

The criterion defined in (7) depends on the unknown initial state x_{t-L}, the unknown disturbance input sequence $d_{t-L:t+T-1}$, the measured output sequence $y_{t-L:t}$ via the cost on $n_{t-L:t}$, and the control input sequence $u_{t-L:t+M-1}$. The control input sequence is composed of two distinct sequences: the (known) past inputs $u_{t-L:t-1}$ that have already been applied, and the future inputs $u_{t:t+M-1}$ that need to be characterized. To select the future inputs $u_{t:t+M-1}$, we optimize (minimize) the criterion (7) with respect to these variables, akin to standard MPC. At a given time $t \in \mathbb{Z}_{\geqslant 0}$, we do not know the values of x_{t-L} and $d_{t-L:t+T-1}$ (and $n_{t-L:t}$, which depend on these), so we optimize the criterion under worst-case assumptions on these variables (i.e., maximize (7)). The optimization (6) is repeated at each time step, i.e., every $T_s = 5$ minutes.

The last two terms in (7) involving d_k and n_k penalize large or unlikely values for the disturbances and noise in the same way that the second term involving u_k penalizes large control inputs. The scalar weights λ_u, λ_d, and λ_n can be tuned to provide the most effective penalties as well as to ensure that there exists a saddle-point solution to the min-max optimization problem (6). For more details on the formulation and stability of this MPC/MHE approach, we refer the reader to [22, 23, 33].

As is common in MPC, at each time t, we use as the control input the first element of the sequence

$$u^*_{t:t+M-1} = \{u^*_t, u^*_{t+1}, u^*_{t+2}, \ldots, u^*_{t+M-1}\}$$

that minimizes (6), leading to the following control law:

$$u_t = u^*_t, \quad \forall t \in \mathbb{Z}_{\geqslant 0}. \tag{9}$$

DOI: 10.1002/oca

At each time t, after the solution to (6) is computed, the control input commanded to the pump is the value of u_t^* rounded down to the nearest integer multiple of the CSII pump-discretization of 0.05 [U] [17]. The portion that is removed when rounding down is then added to the control command given at time $t+1$ in a so-called *carry-over* scheme, which is precisely described in [17].

More details and theoretical results regarding this approach to combine MPC with MHE can be found in [22, 23]. A particular primal-dual-like interior-point method was developed by the authors to numerically solve these optimization problems, and details about this method can be found in [23]. In addition, this MPC/MHE approach allows for the estimation of unknown or uncertain model parameters [34]. Therefore, future work could involve the learning of unknown parameters in the model (2) for, e.g., patient specific (personalized) treatment.

3.2. *State-feedback MPC and Luenberger Observer*

For completeness, we now give a brief overview of the simplified asymmetric MPC/LO approach that we use for comparison. The full MPC/LO approach used in clinical trials is described in detail in [17]. The purpose of this work is to investigate the benefits of the proposed MPC/MHE method with the simplest possible comparison to an existing AP control method; therefore, the version of this MPC/LO approach with which we compare does not include several important safety features that are included in [17] for deployment in clinical trials. These additional features are diurnal BG target ranges and constraints, feed-forward control action following user-initiated meal-announcement, and insulin-on-board constraints. For more details on these additional features of the MPC/LO approach and its performance in trials, we refer the interested reader to [17, 6].

The main conceptual difference between this MPC/LO approach and the MPC/MHE approach described above is that the MPC/MHE approach employs output-feedback, whereas the MPC/LO approach is based on state-feedback. State-feedback control is dependent upon the state estimator whose function is independent of, and unrelated to, the control design. In the MPC/MHE approach, the state estimate and control are computed simultaneously, so they directly affect each other and yield an input that is designed for a worst-case cost outcome. Another difference is that with MPC/LO the asymmetric cost is on the control input rather than the predicted output as with MPC/MHE. This is meant to facilitate decoupled design of the control response to hypoglycemia and hyperglycemia, whereas the asymmetry on the output in the MPC/MHE approach allows both the minimizer and the maximizer to affect the result asymmetrically because the predicted output depends on both u and d. Finally, neither disturbances nor noise are explicitly considered in this MPC/LO approach.

The state estimate $\hat{x}_t$ that is used for control in the MPC/LO approach is found using a linear recursive state estimator known as a Luenberger observer (see, e.g., [35]). This state estimator is given by

$$\hat{x}_{t+1} = A\hat{x}_t + K(y_t - \hat{y}_t) + Bu_t, \qquad \hat{y}_t = C\hat{x}_t, \tag{10}$$

where the gain K is designed as in [17].

We formulate the asymmetric MPC/LO problem as a finite-horizon optimization problem, to be solved at each time t, of the form

$$\min_{u_{t:t+M-1}} J_t(x_t, u_{t:t+M-1}) \tag{11}$$

with cost function

$$J_t(\cdot) \coloneqq \sum_{k=t+1}^{t+T} z_k^2 + \sum_{k=t}^{t+M-1} \left(\hat{R}\hat{u}_k^2 + \check{R}\check{u}_k^2\right), \tag{12}$$

and subject to

$$x_t = \hat{x}_t \tag{13a}$$

$$x_{k+1} = Ax_k + Bu_k \qquad \forall k \in \mathbb{Z}_t^{t+T-1} \tag{13b}$$

DOI: 10.1002/oca

$$y_k = Cx_k \qquad \forall k \in \mathbb{Z}_t^{t+T} \tag{13c}$$
$$u_k \in \mathcal{U} \qquad \forall k \in \mathbb{Z}_t^{t+M-1} \tag{13d}$$
$$u_k = 0 \qquad \forall k \in \mathbb{Z}_{t+M}^{t+T-1} \tag{13e}$$
$$\hat{u}_k = \max(u_k, 0) \qquad \forall k \in \mathbb{Z}_t^{t+M-1} \tag{13f}$$
$$\check{u}_k = \min(u_k, 0) \qquad \forall k \in \mathbb{Z}_t^{t+M-1} \tag{13g}$$
$$z_k = Z(y_k) \qquad \forall k \in \mathbb{Z}_{t+1}^{T} \tag{13h}$$

where $\hat{R}$ and $\check{R}$ are positive scalar weights on the non-negative and non-positive control inputs, respectively. As in [17], we choose the weights to be $\hat{R} = 7000$ and $\check{R} = 100$ in order to conservatively respond to hyperglycemia while encouraging pump attenuation in response to predicted hypoglycemia. As before, only the first element u_t^* of the predicted optimal insulin trajectory is commanded to the pump, and the optimization (11) is repeated at each time step, i.e., every $T_s = 5$ minutes.

Equation (13a) enforces that the initial state is defined as the state estimate from the Luenberger observer (10). Equations (13b)-(13c) enforce the dynamics of the model (2) without considering disturbances or noise. Equation (13d) enforces that the control input belongs to the constraint set $\mathcal{U}$ (as defined in (5)). Equation (13e) ensures that, beyond the control horizon M, the basal rate u_{BASAL} is delivered. Equations (13f)-(13g) facilitate an asymmetric input cost and provide positive and negative deviations of the input u_k from u_{BASAL}. Finally, (13h) provides the cost for output excursions from the desired BG range, where $Z(y_k)$ is defined in (3).

Figure 2 shows the input and output costs used in both the MPC/MHE approach and the MPC/LO approach.

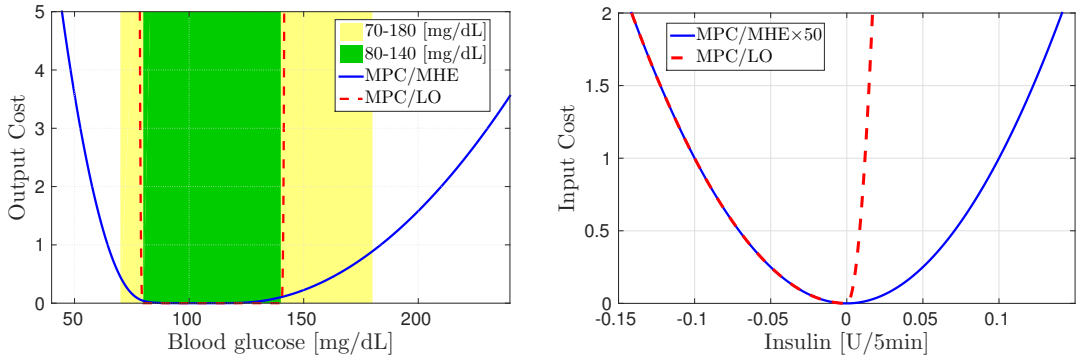

(a) Output costs. The desired and admissible BG ranges are shown in green and yellow, respectively, for reference.

(b) Input costs. The MPC/MHE input cost is multiplied by 50 for comparison because $\check{R}/\lambda_u = 50$.

Figure 2. Output and input costs for MPC/MHE and MPC/LO as given in the first and second terms of (7) and (12), respectively.

In general, solving the optimization problems corresponding to MPC formulations can be nontrivial. Fortunately, the optimization problem corresponding to the MPC/LO approach can be formulated and solved as a quadratic program, and the clinical version of the controller has been implemented and tested on a tablet computer during clinical trials; for details, see [17]. The MPC/MHE approach can be solved very efficiently using a primal-dual-like interior-point method presented in [23]. In both cases, the sample-period $T_s = 5$ minutes is sufficiently long (excessive by multiple orders of magnitude) to compute a solution to the optimization problems.

DOI: 10.1002/oca

4. SIMULATION STUDY

The efficacy of this combined MPC/MHE estimation and control approach is demonstrated via *in-silico* trials of 10 virtual subjects using the commercially available UVA/Padova USFDA accepted metabolic simulator [31]. While we do not present formal stability proofs for either approach in this work, we note that in all simulations performed and presented using the UVA/Padova metabolic simulator resulted in stable behavior. Simulations[†] start at 14:00 and are 28 hours in duration. The simulations begin with two hours of open-loop until 16:00 when the feedback controller is turned on, and simulations run in closed-loop until 18:00 the next day. Every simulation includes three 90 gram carbohydrate (gCHO) meals consumed at 18:30, 07:00, and 13:00, respectively. For most people, 90 gCHO constitutes a large meal, and it happens to be the largest meal allowed in the clinical protocol of [6]. The parameters of both the simulator and controller are time-invariant, so the time of day of meal consumption is irrelevant. We only consider the most challenging case of unannounced meals, meaning the controller has no information about when a meal is consumed, or how large any consumed meal is, and therefore the meal-disturbance is rejected based on CGM feedback only. To further stress the controller, the UVA/Padova simulator includes subjects with parameter values that may be considered beyond the spectrum of plausible values.

We consider a total of 110 simulations. All 10 subjects in the commercially available UVA/Padova metabolic simulator are simulated 11 times: 10 times with different seeds for random CGM additive sensor noise and once with no additive sensor noise. Even without additive sensor noise, the CGM measurements are subject to dynamics and delays that cause it to differ from the true (simulated) BG values. For more details, see [31]. We make no assumptions about the CGM measurement noise, which is, in general, neither zero-mean nor Gaussian. Therefore, we do not introduce constraints on the measurement noise but simply penalize it according to the last term in (7).

4.1. Comparison of MPC/MHE and MPC/LO

The aggregate results for all 110 simulations are shown in Figure 3(a). A zoomed version of these results for the first meal is shown in Figure 3(b). To yield a meaningful comparison, the MPC/MHE approach is tuned specifically to achieve similar hyperglycemic peaks after meal consumption as those achieved by the MPC/LO approach. This facilitates a comparison between the proposed MPC/MHE and benchmark MPC/LO approach, with respect to the other glucose control metrics. In particular, the aggregate results in Figure 3(a) show that the MPC/MHE approach is able to prevent the extremely low BG values that are within the min/max envelope of the MPC/LO approach. In addition, the MPC/MHE approach does not cause a large rebound in BG just before 03:00 as the MPC/LO approach does. However, we see that, on average, BG values are not regulated back to within the desired BG range as soon after a meal is consumed using the MPC/MHE approach. Finally, the hyperglycemic peak after the third meal is noticeably lower for the MPC/MHE approach; this is likely due to the fact that the MPC/MHE approach enforces shorter pump suspensions, resulting in more insulin-on-board, which helps to attenuate the BG response due to the meal. We discuss this further later.

The insulin profiles, shown in the bottom plots of Figure 3, are significantly different. The amount of insulin delivered using the MPC/MHE approach peaks at a lower value after a meal is consumed, but it continues delivering insulin above the basal rate for longer than the MPC/LO approach. Another significant difference is that, after a meal is consumed, the MPC/MHE approach responds more quickly by delivering insulin above the basal rate before the MPC/LO approach does. This is most easily seen in Figure 3(b). This benefit is likely due to the difference in estimation schemes; the Luenberger observer is recursive, which may cause its state estimate to lag slightly when a rapid change in the state occurs. The advantage of this faster insulin delivery achieved with MPC/MHE is quantified in Figure 7 below.

[†]All simulations were performed by Ravi Gondhalekar at the University of California, Santa Barbara (UCSB).

DOI: 10.1002/oca

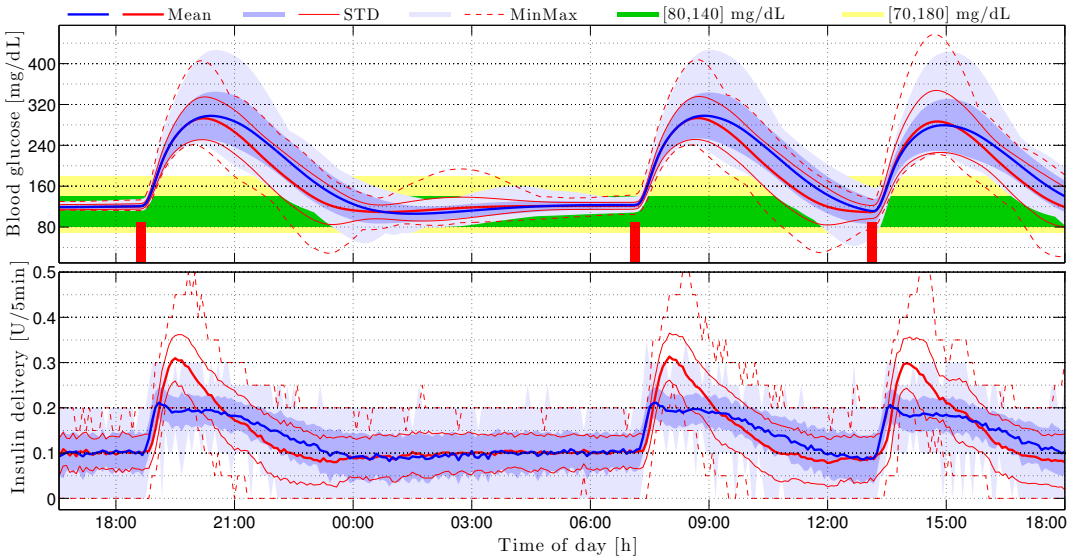

(a) Entire simulation. The red vertical bars at 18:30, 07:00, and 13:00 indicate times a 90 gCHO meal is consumed.

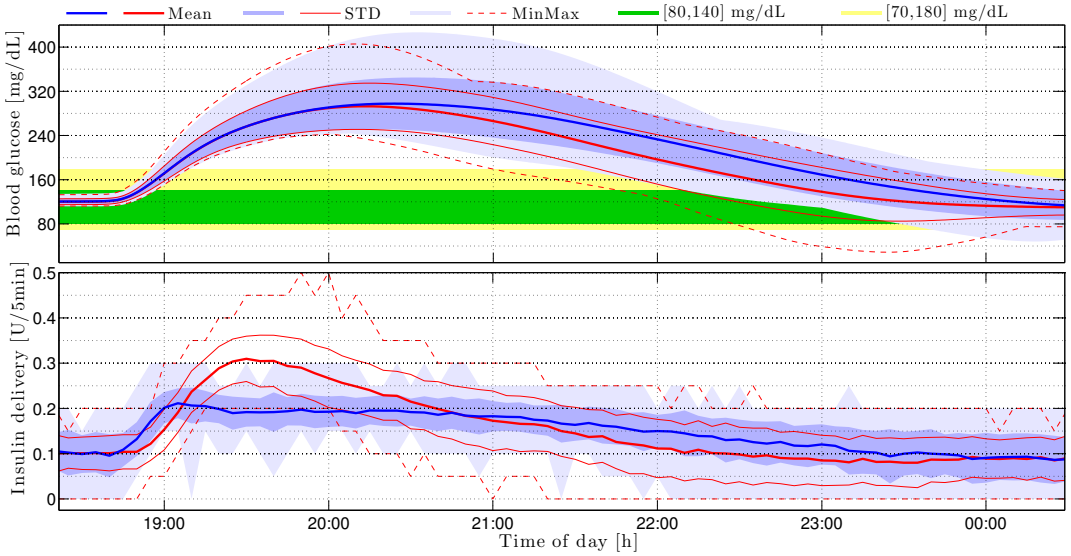

(b) First meal response.

Figure 3. Aggregate results of all 110 simulations for the MPC/MHE approach (blue) and the MPC/LO approach (red). The top sub-plots show the mean BG trajectory as well as its standard deviation and minimum/maximum envelope. The bottom sub-plots show the mean insulin delivered as well as its standard deviation and minimum/maximum envelope.

These features can also be seen, perhaps more clearly, in Figure 4, which shows results for an individual subject for both the MPC/MHE approach and the MPC/LO approach. This particularly challenging virtual subject was chosen to highlight the differences between the approaches. For both the MPC/MHE and MPC/LO approaches, Figure 4 shows the actual BG trajectories in the top plot and the insulin delivered in the bottom plot. The MPC/MHE approach tends to keep BG levels slightly higher but effectively mitigates the extreme hypoglycemia experienced using the MPC/LO approach. The MPC/LO approach clearly suspends the pump (i.e., delivers 0 [U] of insulin) much longer than the MPC/MHE approach in the face of impending hypoglycemia. This results in a larger rebound in the BG for the MPC/LO approach after 00:00 as well as a higher peak after the third

DOI: 10.1002/oca

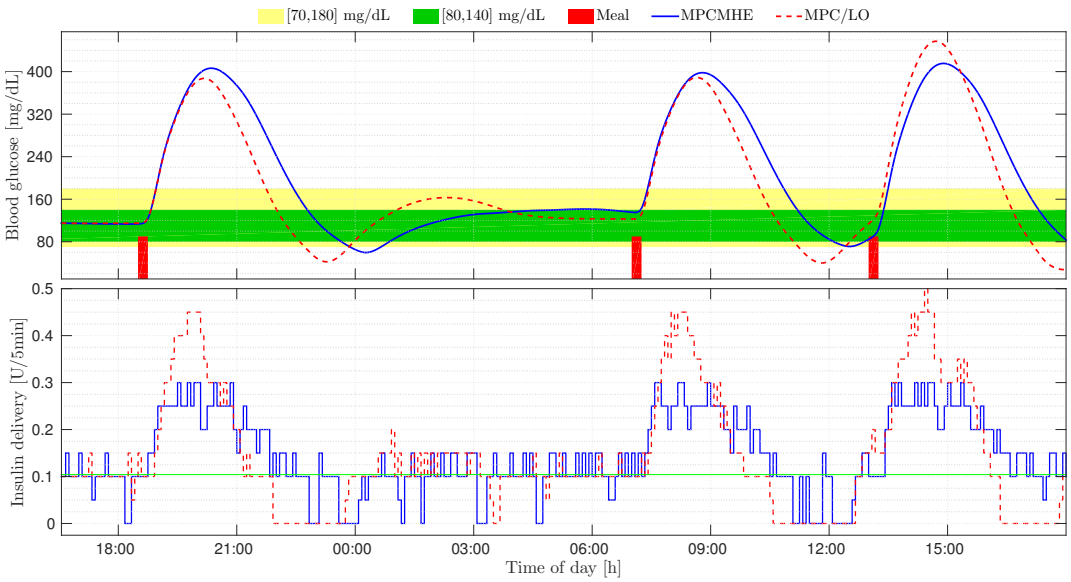

Figure 4. Results for Subject #7 with random additive noise seed 2. The top plot shows the BG for both the MPC/MHE approach (blue solid) and the MPC/LO approach (red dashed). Similarly, the bottom plot shows the insulin delivered for each approach as well as the basal insulin rate (green solid).

meal. Finally, the bottom plot shows that the MPC/MHE approach commands insulin to be delivered above the basal rate earlier than the MPC/LO approach after meal consumption.

Another way to present aggregate performance of a controller for the AP problem is to consider Control-Variability Grid Analysis (CVGA) plots as described in [36]. Figures 5(a) and 5(b) show the CVGA plots for our MPC/MHE approach as well as the MPC/LO approach, respectively, for all 110 simulations. The black dots represent each simulation's minimum (horizontal axis) and maximum (vertical axis) BG values with the highest and lowest 2.5% removed. The large blue dot denotes the arithmetic mean of the individual black dots, and the blue circle has a radius of the standard deviation of the distances of each individual dot.

The CVGA plots in Figure 5 show that our MPC/MHE approach has a mean value that is shifted to the left and just slightly higher than the mean value of the MPC/LO approach. This means that our MPC/MHE approach is effective at keeping subjects from experiencing dangerously low BG levels with the caveat that they may experience slightly higher glucose levels on average. This comparison is easy to see in Figure 4 for a single subject. In addition, the standard deviation for the MPC/MHE approach is significantly smaller than the standard deviation for the MPC/LO approach. A reduction in the CVGA standard deviation implies that the same controller is affected less by inter-subject variability. The resulting number of simulations in each of the CVGA zones, as well as the mean and standard deviation values, are given in Table I for both approaches. These statistics indicate that the MPC/LO approach has 11 black dots in the upper right-hand corner superimposed.

4.2. Quantifying these results

In this section we quantify the advantages of using the MPC/MHE approach over the MPC/LO approach. Specifically, the MPC/MHE approach results in: 1) fewer hypoglycemic events with the same number of hyperglycemic events, 2) fewer and shorter insulin pump suspensions, helping to smooth BG trajectories, and 3) accelerated insulin delivery in response to meal consumption. The main drawback of using the MPC/MHE approach is that the BG values are slightly higher on average.

Table I contains the aggregate results for both approaches. The first set of rows shows the time-in-range percentages of two BG intervals and several thresholds. As we noted before, the MPC/LO approach keeps the BG within the desired range a larger percentage of the time and also results

Prepared using ocaauth.cls
DOI: 10.1002/oca

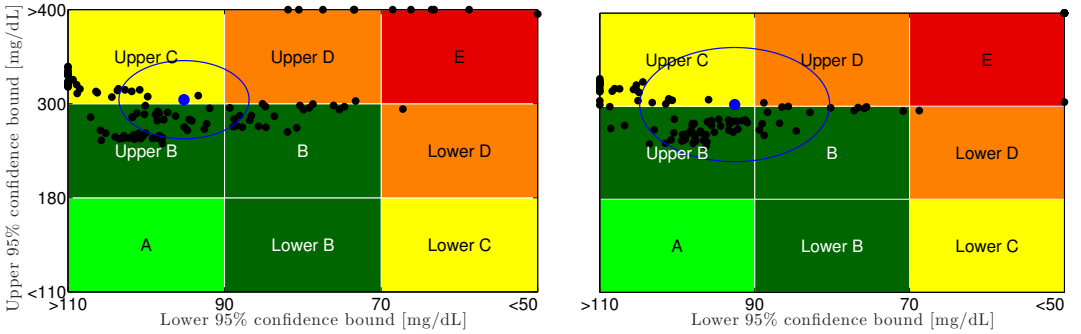

(a) MPC/MHE. Number of 110 simulations in each zone (A,B,C,D,E)=(0,64,33,7,6).

(b) MPC/LO. Number of 110 simulations in each zone (A,B,C,D,E)=(0,64,32,2,12). Several points are superimposed, e.g., in zone E.

Figure 5. CVGA plots for 110 simulations. The circles are centered on the mean with radius equal to the standard deviation. Related statistics are provided in Table I.

in less time above hyperglycemic values. The MPC/MHE approach, on the other hand, results in significantly less time below hypoglycemic thresholds. Both approaches may be tuned to adjust these values, but in this work, we tuned the MPC/MHE approach specifically to achieve comparable hyperglycemic peaks as the MPC/LO approach in order to contrast other features of the controllers.

The second set of rows in Table I list the number of simulations for which BG values are above or below several thresholds. The corresponding number of subjects (out of the 10 subjects in the simulator) that experience those BG values are given in parentheses. The third set of rows lists the number of events for which BG values are above or below those same thresholds. The two control strategies were tuned to achieve close to equal BG peaks after meal consumption, and therefore the two approaches' control performance with respect to hyperglycemic statistics are very similar. However, using the MPC/MHE approach results in half as many simulations experiencing hypoglycemia of less than 60 [mg/dL] and *far* fewer hypoglycemic events. Histograms for the number of hyperglycemic and hypoglycemic events are given in Figure 6(a).

The fourth set of rows in Table I shows the number of pump suspensions that last longer than particular lengths of time. A histogram of these results is shown in Figure 6(b). The MPC/MHE approach results in fewer suspensions of lengths greater than 15 and 30 minutes and results in no pump suspensions longer than 60 minutes. This is an advantage because, while suspending the pump is important in order to attenuate predicted hypoglycemic BG values and safeguard from dangerous outcomes, long pump suspensions can deteriorate overall performance as less insulin is present in the body, causing BG values to rebound or peak higher after a meal is consumed. Both of these issues can be seen in the aggregate results in Figure 3(a) and the individual results in Figure 4 where a long pump suspension, as commanded by the MPC/LO approach, causes BG values to rebound after the first meal and peak higher after the third meal.

The fifth set of rows in Table I gives the number of UCSB Health Monitoring System (HMS) alarms [37] and number of simulations that experience HMS alarms. The MPC/MHE approach causes significantly fewer alarms than the MPC/LO approach. Minimizing the number of alarms is important when implementing these controllers because if alarms go off too frequently, subjects may experience "alarm fatigue" and ignore the alarms. The sixth set of rows in Table I gives the numerical results corresponding to the CVGA plots in Figure 5. The seventh set of rows gives the mean, minimum, and maximum BG values for each approach, as well as the corresponding p-values from a paired t-test. The MPC/MHE approach results in a slightly higher mean BG but also a higher minimum BG. Interestingly, the MPC/MHE approach produces a very slightly lower maximum BG. The eighth set of rows gives the Low Blood Glucose Index (LBGI) and High Blood Glucose Index (HGBI), as computed according to [12], and the corresponding p-values. As expected, the MPC/MHE approach results in a lower LBGI but a higher HBGI. Finally, the last row gives the total amount of insulin delivered using each approach averaged over all 110 simulations as well as

DOI: 10.1002/oca

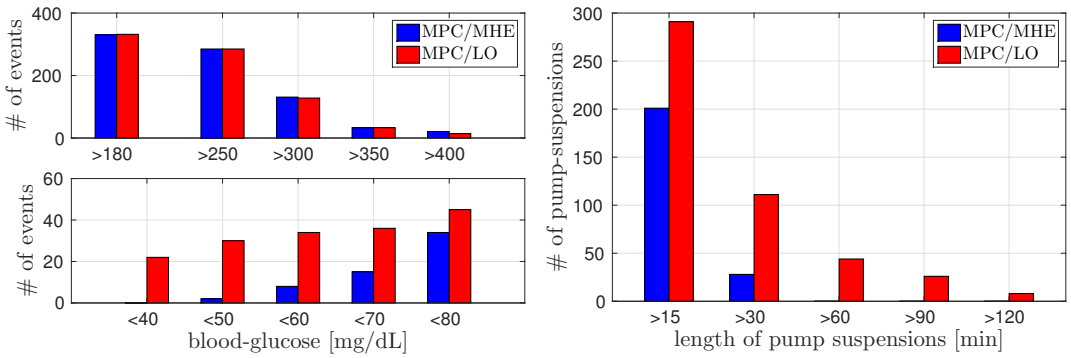

(a) Number of hyperglycemic and hypoglycemic events.

(b) Number of pump suspensions.

Figure 6. Histograms for the number of hyperglycemic and hypoglycemic events as well as the number of pump suspensions for the MPC/MHE approach (blue) and the MPC/LO approach (red).

the standard deviation, minimums and maximums, and p-values. The MPC/MHE approach delivers less insulin than the MPC/LO approach; therefore, it is not surprising that the MPC/MHE results in slightly higher mean BG.

The last advantage, and one that is not quantified in Table I, is that the MPC/MHE approach delivers insulin more quickly after a meal. This was mentioned when discussing the aggregate responses after the first meal shown in Figure 3(b) and is precisely quantified in Figure 7. For reference, the basal insulin rate is shown in Figure 7 and increases at a rate of 0.1026 [U/5min]. On average, BG begins to rise about 10 minutes after a meal is consumed. After 20 minutes, the MPC/MHE approach begins to deliver insulin at a rate higher than the basal rate. The MPC/LO approach, on the other hand, does not deliver insulin at a rate higher than the basal rate until 30 minutes after a meal is consumed. Consequently, the MPC/MHE approach delivers more insulin compared to the MPC/LO approach for the first 55 minutes after a meal is consumed, after which time the MPC/LO approach continues delivering insulin at a higher rate. Moreover, the mean BG is lower for the MPC/MHE approach until about 105 minutes after meal consumption even though it starts out slightly higher than the BG for the MPC/LO approach before a meal. This faster response to increasing BG values may be due to using an MHE-like state estimator as opposed to a Luenberger observer because the Luenberger observer computes the estimates recursively and, therefore, may produce a lagging state estimate if the state is rapidly changing. This phenomenon is also found in [21] when specifically comparing the results of a state-feedback MPC strategy using both a Luenberger observer and an MHE for estimating BG. The MPC/MHE approach does not, however, cumulatively deliver as much insulin as the MPC/LO approach, so BG values stay slightly higher for longer using the MPC/MHE approach.

5. CONCLUSIONS

We presented a new estimation and control approach for regulating BG in T1DM. This approach simultaneously performs Model Predictive Control and Moving Horizon Estimation in a single min-max optimization problem to form a feedback controller that results in elevated cost-conservatism with respect to disturbances. This combined MPC/MHE approach incorporates an asymmetric output cost penalizing "riskier" low BG values more severely than high BG values. We compared this approach to a state-feedback MPC approach that utilized a Luenberger observer for state estimation and incorporated an asymmetric input cost in order to decouple the controller's response to low versus high BG values. This MPC/LO approach is a simplified version of an estimation and control approach that has been successfully tested in clinical trials.

Both of these control and estimation approaches were evaluated with *in-silico* studies utilizing a metabolic simulator. In 110 simulations of 10 virtual subjects, we found that while the MPC/MHE approach keeps BG values slightly higher on average, it successfully reduces the number of

DOI: 10.1002/oca

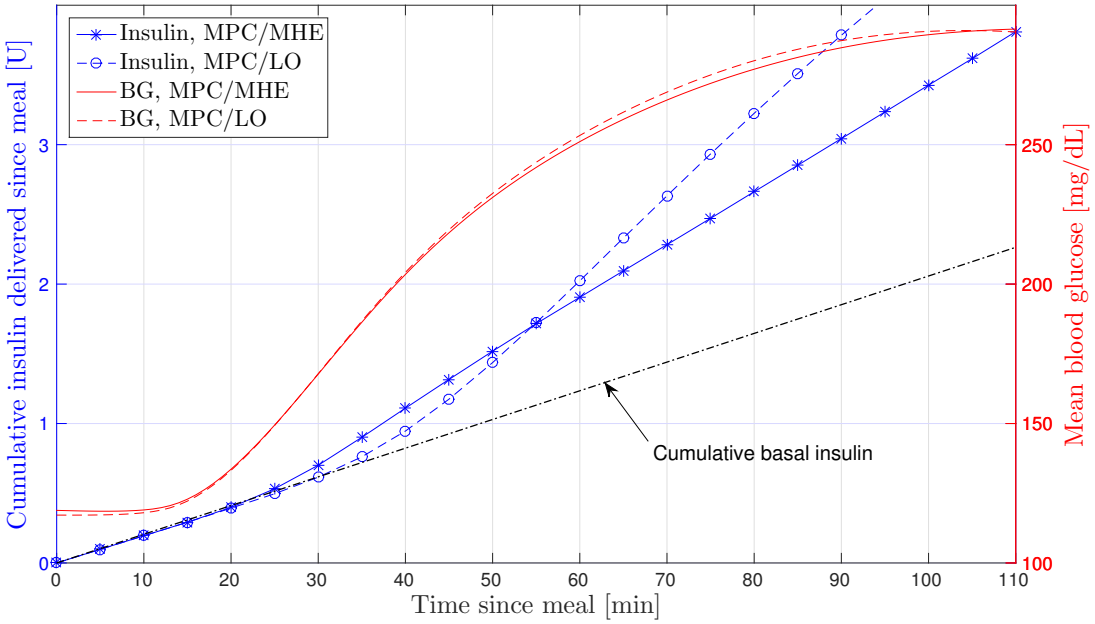

Figure 7. Cumulative insulin delivered (blue) and mean BG (red) since a meal consumption for both MPC/MHE and MPC/LO approaches averaged over all three meals and 110 simulations.

hypoglycemic events without increasing the number of hyperglycemic events, it delivers insulin sooner in response to meal consumption, and it commands shorter insulin pump suspensions, which results in smoother BG trajectories. Therefore, this MPC/MHE approach may be advantageous for the feedback control of an AP for the treatment of T1DM.

6. ACKNOWLEDGMENTS

This material is based upon work partially supported by the National Science Foundation under Grant No. ECCS-1608880. The authors thank Dr. F. J. Doyle III and Dr. E. Dassau, both of Harvard University, for their support, and for providing the environment that lead to this work. The authors acknowledge that access to the UVA/Padova metabolic simulator was provided by an agreement with Prof. C. Cobelli (University of Padova) and Prof. B. P. Kovatchev (UVA) for research purposes. All simulations using the metabolic simulator were performed by Ravi Gondhalekar at UCSB. Ravi Gondhalekar acknowledges funding provided by the National Institutes of Health: DP3DK094331, R01DK085628.

REFERENCES

1. Haidar A. The artificial pancreas: How closed-loop control is revolutionizing diabetes. *IEEE Control Systems* October 2016; **36**(5):28–47.
2. Cobelli C, Renard E, Kovatchev B. Artificial pancreas: Past, present, future. *Diabetes* November 2011; **60**:2672–2682.
3. Doyle III FJ, Huyett LM, Lee JB, Zisser HC, Dassau E. Closed-loop artificial pancreas systems: Engineering the algorithms. *Diabetes Care* May 2014; **37**:1191–1197.
4. Grosman B, Dassau E, Zisser HC, Jovanovič L, Doyle III FJ. Zone model predictive control: A strategy to minimize hyper- and hypoglycemic events. *Journal of Diabetes Science and Technology* July 2010; **4**(4):961–975.
5. Breton M, Farret A, Bruttomesso D, Anderson S, Magni L, Patek S, Dalla Man C, Place J, Demartini S, Del Favero S, *et al.*. Fully integrated artificial pancreas in type 1 diabetes: Modular closed-loop glucose control maintains near normoglycemia. *Diabetes* September 2012; **61**:2230–2237.
6. Dassau E, Brown SA, Basu A, Pinsker JE, Kudva YC, Gondhalekar R, Patek S, Lv D, Schiavon M, Lee JB, *et al.*. Adjustment of open-loop settings to improve closed-loop results in type 1 diabetes: A multicenter randomized trial. *J. Clinical Endocrinology & Metabolism* October 2015; **100**(10):3878–3886.

DOI: 10.1002/oca

7. Huyett LM, Ly TT, Forlenza GP, Reuschel-DiVirgilio S, Messer LH, Wadwa RP, Gondhalekar R, Doyle III FJ, Pinsker JE, Maahs DM, *et al.*. Outpatient closed-loop control with unannounced moderate exercise in adolescents using zone model predictive control. *Diabetes Technology & Therapeutics* June 2017; **19**(6):331–339.
8. Hovorka R. Continuous glucose monitoring and closed-loop systems. *Diabetic Medicine* January 2005; **23**:1–12.
9. Bequette BW. A critical assessment of algorithms and challenges in the development of a closed-loop artificial pancreas. *Diabetes Technology and Therapeutics* 2005; **7**(1):28–47.
10. Parker RS, Doyle III FJ, Peppas NA. A model-based algorithm for blood glucose control in type I diabetic patients. *IEEE Transactions on Biomedical Engineering* February 1999; **46**(2):148–157.
11. Hovorka R, Canonico V, Chassin LJ, Haueter U, Massi-Benedetti M, Federici MO, Pieber TR, Shaller HC, Schaupp L, Vering T, *et al.*. Nonlinear model predictive control of glucose concentration in subjects with type 1 diabetes. *Physiological Measurement* 2004; **25**:905–920.
12. Magni L, Raimondo D, Dalla Man C, Nicolao GD, Kovatchev B, Cobelli C. Model predictive control of glucose concentration in type I diabetic patients: An in silico trial. *Biomedical Signal Processing and Control* May 2009; **4**:338–346.
13. Morari M, Lee JH. Model predictive control: past, present and future. *Computers & Chemical Engineering* 1999; **23**(4):667–682.
14. Rawlings JB, Mayne DQ. *Model Predictive Control: Theory and Design*. Nob Hill Publishing: Madison, WI, USA, 2009.
15. Qin SJ, Badgwell TA. A survey of industrial model predictive control technology. *Control Engineering Practice* 2003; **11**(7):733–764.
16. Rawlings JB, Bakshi BR. Particle filtering and moving horizon estimation. *Computers & Chemical Engineering* 2006; **30**(10):1529–1541.
17. Gondhalekar R, Dassau E, Doyle III FJ. Periodic zone-MPC with asymmetric costs for outpatient-ready safety of an artificial pancreas to treat type 1 diabetes. *Automatica* September 2016; **71**:237–246.
18. Gondhalekar R, Dassau E, Doyle III FJ. MPC design for rapid pump-attenuation and expedited hyperglycemia response to treat T1DM with an artificial pancreas. *American Control Conference (ACC)*, 2014; 4224–4230.
19. Gondhalekar R, Dassau E, Doyle III FJ. Velocity-weighting to prevent controller-induced hypoglycemia in MPC of an artificial pancreas to treat T1DM. *American Control Conference (ACC)*, 2015; 1635–1640.
20. Gondhalekar R, Dassau E, Zisser HC, Doyle III FJ. Periodic-zone model predictive control for diurnal closed-loop operation of an artificial pancreas. *Journal of Diabetes Science and Technology* November 2013; **7**:1446–1460.
21. Lee JJ, Gondhalekar R, Doyle III FJ. Design of an artificial pancreas using zone model predictive control with a moving horizon state estimator. *53rd IEEE Conference on Decision and Control (CDC)*, 2014; 6975–6980.
22. Copp DA, Hespanha JP. Nonlinear output-feedback model predictive control with moving horizon estimation. *53rd IEEE Conference on Decision and Control (CDC)*, 2014; 3511–3517.
23. Copp DA, Hespanha JP. Simultaneous nonlinear model predictive control and state estimation. *Automatica* March 2017; **77**:143–154.
24. Boiroux D. Model predictive control algorithms for pen and pump insulin administration. PhD Thesis, Technical University of Denmark 2012.
25. Harvey RA, Dassau E, Bevier WC, Seborg DE, Jovanovič L, Doyle III FJ, Zisser HC. Clinical evaluation of an automated artificial pancreas using zone-model predictive control and health monitoring system. *Diabetes Technology and Therapeutics* 2014; **16**(6):348–357.
26. Cobelli C, Dalla Man C, Sparacino G, Magni L, De Nicolao G, Kovatchev BP. Diabetes: Models, signals, and control. *IEEE Reviews in Biomedical Engineering* 2009; **2**:54–96.
27. van Heusden K, Dassau E, Zisser HC, Seborg DE, Doyle III FJ. Control-relevant models for glucose control using a priori patient characteristics. *IEEE Transactions on Biomedical Engineering* July 2012; **59**(7):1839–1849.
28. Colmegna P, Sánchez Peña RS. Analysis of three T1DM simulation models for evaluating robust closed-loop controllers. *Computer Methods and Programs in Biomedicine* 2014; **113**:371–382.
29. Ellingsen C, Dassau E, Zisser HC, Grosman B, Percival MW, Jovanovič L, Doyle III FJ. Safety constraints in an artificial pancreatic β cell: An implementation of model predictive control with insulin on board. *Journal of Diabetes Science and Technology* May 2009; **3**:536–544.
30. Turksoy K, Samadi S, Feng J, Littlejohn E, Quinn L, Cinar A. Meal detection in patients with type 1 diabetes: a new module for the multivariable adaptive artificial pancreas control system. *IEEE journal of biomedical and health informatics* 2016; **20**(1):47–54.
31. Kovatchev BP, Breton M, Dalla Man C, Cobelli C. In silico preclinical trials: A proof of concept in closed-loop control of type 1 diabetes. *Journal of Diabetes Science and Technology* January 2009; **3**:44–55.
32. Walsh J, Roberts R. *Pumping Insulin*. 4th edn., Torrey Pines Press: San Diego, CA, USA, 2006.
33. Copp DA, Hespanha JP. Conditions for saddle-point equilibria in output-feedback MPC with MHE. *American Control Conference (ACC)*, 2016; 13–19.
34. Copp DA, Hespanha JP. Addressing adaptation and learning in the context of model predictive control with moving horizon estimation. *Control of Complex Systems: Theory and Applications*. chap. 6, Butterworth-Heinemann, 2016; 187–209.
35. Levine WS ((ed.)). *The control handbook*. 2nd edn., CRC Press.: Boca Raton, FL, USA, 2011.
36. Magni L, Raimondo DM, Dalla Man C, Breton M, Patek S, Nicolao GD, Cobelli C, Kovatchev BP. Evaluating the efficacy of closed-loop glucose regulation via control-variability grid analysis. *Journal of Diabetes Science and Technology* July 2008; **2**:630–635.
37. Harvey RA, Dassau E, Zisser HC, Seborg DE, Jovanovič L, Doyle III FJ. Design of the health monitoring system for the artificial pancreas: Low glucose prediction module. *Journal of Diabetes Science and Technology* November 2012; **6**:1345–1354.

Table I. Aggregate results for the two comparisons considered.

		MPC/MHE	MPC/LO
BG [mg/dL] % time	$\in [80, 140]$	45.47	49.19
	$\in [70, 180]$	56.62	61.24
	< 80	1.05	1.85
	< 70	0.39	1.30
	< 60	0.13	0.99
	< 50	0.03	0.68
	< 40	0.00	0.34
	> 180	42.99	37.46
	> 250	20.84	17.53
	> 300	7.70	5.98
	> 350	1.93	1.43
	> 400	0.58	0.45
# Simulations (# Subjects) with BG [mg/dL]	< 80	21 (3)	20 (2)
	< 70	10 (2)	14 (2)
	< 60	6 (1)	12 (2)
	< 50	1 (1)	12 (2)
	< 40	0 (0)	12 (2)
	> 180	110 (10)	110 (10)
	> 250	109 (10)	108 (10)
	> 300	53 (7)	53 (7)
	> 350	11 (1)	11 (1)
	> 400	11 (1)	11 (1)
# Events BG [mg/dL]	< 80	34	45
	< 70	15	36
	< 60	8	34
	< 50	2	30
	< 40	0	22
	> 180	330	332
	> 250	285	285
	> 300	131	128
	> 350	33	33
	> 400	21	14
# Pump Suspensions	$\geqslant 15$ min	201	291
	$\geqslant 30$ min	28	111
	$\geqslant 60$ min	0	44
	$\geqslant 90$ min	0	26
	$\geqslant 120$ min	0	8
	$\geqslant 150$ min	0	0
# HMS Alarms		37	95
# Simulations with HMS Alarms		19	23
CVGA zone count: A		0	0
CVGA zone count: B		64	64
CVGA zone count: C		33	32
CVGA zone count: D		7	2
CVGA zone count: E		6	12
CVGA circle radius		8.31	12.26
BG mean: mean$\pm$std [min,max] ($P < 0.01$)		180$\pm$18.92 [152,219]	171$\pm$14.90 [148,201]
BG min: mean$\pm$std [min,max] ($P < 0.01$)		94$\pm$16.72 [43,122]	89$\pm$23.65 [22,121]
BG max: mean$\pm$std [min,max] ($P = 0.13$)		307$\pm$47.18 [247,427]	307$\pm$53.62 [246,457]
LBGI: mean$\pm$std [min,max] ($P = 0.14$)		0.17$\pm$0.29 [0.00,1.97]	0.47$\pm$1.08 [0.00,4.51]
HBGI: mean$\pm$std [min,max] ($P < 0.01$)		10.87$\pm$3.74 [5.47,19.47]	9.36$\pm$2.95 [4.84,14.28]
Total Daily Insulin [U]: mean$\pm$std [min,max] ($P = 0.67$)		41.4$\pm$6.6 [32.7,57.3]	42.5$\pm$7.1 [33.1,59.5]

DOI: 10.1002/oca